



OPEN

SUBJECT AREAS:

ATMOSPHERIC
DYNAMICS

PALAEOCLIMATE

^{18}O depletion in monsoon rain relates to large scale organized convection rather than the amount of rainfall

P. R. Lekshmy, M. Midhun, R. Ramesh & R. A. Jani

Geosciences Division, Physical Research Laboratory, Ahmedabad – 380009, India.

Received
3 February 2014Accepted
19 June 2014Published
11 July 2014Correspondence and
requests for materials
should be addressed to
P.R.L. (lekshmy@prl.
res.in)

Oxygen isotopic variations in rainfall proxies such as tree rings and cave calcites from South and East Asia have been used to reconstruct past monsoon variability, mainly through the amount effect: the observed ^{18}O depletion of rain with increasing amount, manifested as a negative correlation of the monthly amount of tropical rain with its $\delta^{18}\text{O}$, both measured at the same station. This relation exhibits a significant spatial variability, and at some sites (especially North-East and peninsular India), the rainfall proxies are not interpretable by this effect. We show here that relatively higher ^{18}O -depletion in monsoon rain is not related necessarily to its amount, but rather, to large scale organized convection. Presenting $\delta^{18}\text{O}$ analyses of ~654 samples of daily rain collected during summer 2012 across 9 stations in Kerala, southern India, we demonstrate that although the cross correlations between the amounts of rainfall in different stations is insignificant, the $\delta^{18}\text{O}$ values of rain exhibit highly coherent variations (significant at $P = 0.05$). Significantly more ^{18}O -depletion in the rain is caused by clouds only during events with a large spatial extent of clouds observable over in the south eastern Arabian Sea.

Stable oxygen isotopic ($\delta^{18}\text{O}$) variations of proxies (*e.g.*, cellulose of annual growth rings of trees^{1,2} and cave calcites^{3,4}) of past precipitation are decoded mainly using the significant negative correlation between the amount of monthly rain and its $\delta^{18}\text{O}$, known as the ‘amount effect’. This effect is observed^{5–7} in the tropics as typically $\sim -1.5\%$ per 100 mm increase in the monthly precipitation. There is, however, a large spatial variation⁸, because of varying cloud condensation processes and their interaction with ambient atmospheric moisture. The preferential removal of heavier water isotopologues (H_2^{18}O , and HD^{16}O) from the cloud vapour during condensation, and of the lighter isotopologue (H_2^{16}O) during rain evaporation during descent, are known to produce, respectively, ^{18}O (also D)-depleted cloud vapour and ^{18}O (also D)-enriched precipitation. The ^{18}O -depleted water vapour which reaches the sub-cloud layer along with the intense convective down-drafts subsequently moves back to the cloud along with the updrafts. This feedback has been suggested to strengthen the amount effect⁹. Though significant amount effect has been observed in the inland stations of India (*e.g.*, GNIP data for Delhi and reported data for Jarsuguda⁷), recent studies over a few Indian sites under the influence of the Indian Summer Monsoon (ISM) rainfall such as Mangalore, Kozhikode and Cherrapunji show either a lack of amount effect or significant reversed amount effect^{10–12} (*i.e.*, a positive correlation between rain amount and its $\delta^{18}\text{O}$).

South western India (Kerala) gets the first rains in India during ISM, from the moist air masses originating in the southern Indian Ocean and the Arabian Sea and the rainfall is well modulated by the 30–60 day mode of intra seasonal oscillations of ISM^{13–15}. $\delta^{18}\text{O}$ of ISM rain here has the advantage of minimal alteration by continental recycled water (*e.g.*, soil re-evaporation and transpiration from vegetation), and thus could be a good site for examining characteristics of the moisture source and the effect of cloud processes on the $\delta^{18}\text{O}$ of monsoon rain. Daily rain was collected at 9 stations (Fig. 1) between ~ 8 to 13°N , ~ 75 to 77.5°E and 0 to 850 m above sea level (above m.s.l) during mid of May to October, 2012. All the stations are located to the west of the Western Ghats (which has a maximum height of ~ 2700 m above m.s.l in Kerala). On an average, 73 events were sampled at each station, barring events of less than 2 mm/day rain, with a total of 654 samples from all stations. Seasonal total rain during 2012 over Kerala was 24% less than its climatological average value (~ 2040 mm)¹⁶, but individual stations recorded both higher and lower values than their respective climatological means.

In Fig. 2, time series of rainfall (2a), the corresponding rain $\delta^{18}\text{O}$ (2b) are plotted. The daily rainfall over the stations varies from 0 to 263 mm whereas the rainfall $\delta^{18}\text{O}$ varies from 0.3 to -9.7% from the onset to the withdrawal of the monsoon; the amount weighted average $\delta^{18}\text{O}$ of all the stations is $-2.8 \pm 1.6\%$. There exists a large spatiotemporal variability in the daily rainfall; whereas the $\delta^{18}\text{O}$ values of rain are significantly coherent at all

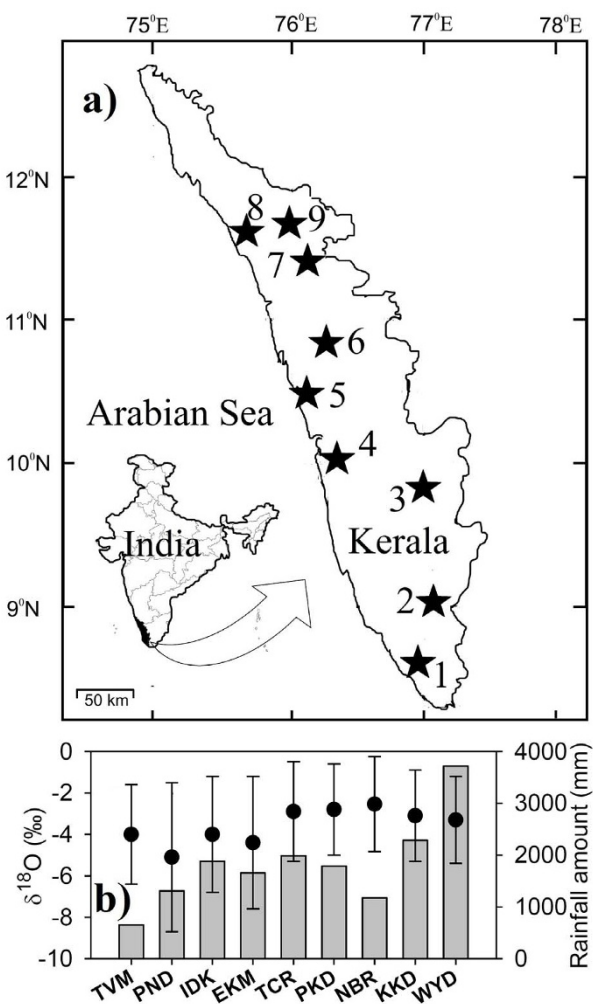


Figure 1 | Sample locations and the amounts & $\delta^{18}\text{O}$ of rain.

(a) Locations: 1- Thiruvananthapuram (TVM, 53 m asl), 2- Ponmudi (PND, 780 m asl), 3- Idukki (IDK, 700 m asl), 4- Ernakulam (EKM, 6 m asl), 5- Thrissur (TCR 12 m asl), 6- Palakkad (erstwhile Palghat) (PKD, 26 m asl), 7- Nilambur (NBR, 35 m asl), 8- Kozhikode (KKD, 30 m asl), 9- Wayanadu (WYD, 800 m asl), plotted using licensed CorelDRAW.

(b) Total rainfall (mm, vertical bars) during Jun-Oct and the corresponding seasonal average $\delta^{18}\text{O}$ (filled circles) with 1σ spread, over each station, plotted using licensed Sigma Plot.

the stations (linear cross-correlation coefficients of rain in different stations are mostly insignificant, while those of $\delta^{18}\text{O}$ of rain between stations are highly significant, as shown in supplementary Table 1). Also, the seasonal average of rainfall $\delta^{18}\text{O}$ in all stations agree within one standard deviation, whereas the total rainfall values show a large variation, with a general increasing trend towards the North (Fig. 1b), with the exception of NBR, located leeward. The spatial variation of the amount of rainfall is induced by the changing orography. The orographic features of Western Ghats play a significant role in modulating the ISM rain, since the mountain ranges are perpendicular to the prevailing ISM winds¹⁷. This coherent pattern of $\delta^{18}\text{O}$ is consistent with the idea that the rain at all the stations is derived from a single vapour mass, when clouds have a large spatial extent over the region. When we regress the monthly mean $\delta^{18}\text{O}$ values of each station with the corresponding monthly values of rainfall, we find that there is no significant correlation. This means that the ‘amount effect’ according to the prevailing definition does not exist in the region.

Gadgil (2003) noted that OLR values significantly less than 240 W/m^2 and SST greater than 27.5°C is indicative of large scale

organised convection¹⁴. Hovmöller diagram *i.e.*, latitude versus time plot of Outgoing Longwave Radiation, OLR) averaged over $65\text{--}77.5^\circ\text{E}$, (Fig. 2c) indicates the relevance of organised convective activity, in determining the temporal variability of rain $\delta^{18}\text{O}$; relatively higher ^{18}O -depletion is seen to correspond mainly with the presence of clouds over larger spatial extent (highlighted by arrows). Four such events are observed from the first day of the monsoon season until the mid-July. During July 15 to August 5, spatial extent of clouds is limited, yet continuous rain is recorded in most stations with a peak during July 25th. The average amount weighted $\delta^{18}\text{O}$ of rain during this period is $-1.3 \pm 0.3\text{‰}$, with no corresponding ^{18}O -depletion with the increased rainfall, shows that the rainfall $\delta^{18}\text{O}$ is independent of rainfall amount. From August 6th onwards the movement of another large cloud cover established: 5–6 additional, high ^{18}O -depletion events are then recorded. A linear correlation coefficient of 0.69 ($P < 0.001$) is observed between the amount weighted mean $\delta^{18}\text{O}$ with the OLR over the $5^\circ\text{N}\text{--}12.5^\circ\text{N}$ and $67.5^\circ\text{E}\text{--}75^\circ\text{E}$ grid box (Supplementary Fig. 1a) till monsoon withdrawal. Thus the pronounced signatures of organised cloud activity are well captured as high ^{18}O depletion in rain.

Thus, if $\delta^{18}\text{O}$ of rain is unrelated to the local rain amount and it is related to large scale convection, then $\delta^{18}\text{O}$ values of rain should be comparable with large scale rain as measured by TRMM (Tropical Rainfall Measuring Mission). The difference in the spatial patterns of TRMM derived rainfall and OLR during high and low ^{18}O -depletion rain events (*i.e.* events not associated with large scale convection) are shown in Fig. 3. Intense rains (Fig. 3b) from clusters of clouds (Fig. 3d) with a large spatial extent over the eastern Arabian Sea, including southern peninsular India, are observed during high ^{18}O -depletion rain events. In contrast, low ^{18}O -depletion rain events (Fig. 3a) are characterized by isolated clouds with smaller spatial extent (Fig. 3c). The average OLR values over the region of convection ($5^\circ\text{N}\text{--}12.5^\circ\text{N}$ and $67.5^\circ\text{E}\text{--}75^\circ\text{E}$ grid box) during high and low ^{18}O -depletion events are $180 \pm 19 \text{ W/m}^2$ and $235 \pm 19 \text{ W/m}^2$, respectively. The corresponding average TRMM rainfall values for the same are $15 \pm 7 \text{ mm/day}$ and $2 \pm 4 \text{ mm/day}$, respectively. Thus, the OLR and TRMM rainfall are significantly different during low and high ^{18}O -depletion events. Presence of clouds with large spatial extent leads to the higher ^{18}O -depletion because (i) fresh condensate is enriched in ^{18}O relative to the vapour according to the Rayleigh model, and so the increased condensation (higher rain amount) reduces ^{18}O in the rain, (ii) rain drops re-evaporate to a lesser extent at the cloud base due to higher ambient humidity and thus less enrichment of ^{18}O compared to events of lesser rain; and (iii) unsaturated downdraft vapour and re-evaporated vapour (both relatively depleted in ^{18}O) during rain events feed the sub-cloud layer vapour^{8,18,19}, which will be taken into the convective clouds through updraft and thereby the rain is further depleted⁹ in ^{18}O .

Strong convection usually occurs in association with strong mid tropospheric convergence of moist air and thus vertical velocity too is a good surrogate for convective activity. Back-trajectory analysis to the mean location ($\sim 10.5^\circ\text{N}$, 76.5°E) of the sampling stations shows (Fig. 4b) an upward motion of air masses during events of higher ^{18}O -depletion, while downward or horizontal wind motion is seen during low ^{18}O -depletion rain events. The average trajectory height during low ^{18}O -depletion events is $\sim 2 \text{ km}$, and air parcels do not move vertically up when they reach Kerala; in contrast, during high ^{18}O -depletion events, the average trajectory height is below 1.5 km . This enables effective pick up of additional moisture from the sub-cloud layer and the warm ocean below, before ascending over the rainfall site. Between rain $\delta^{18}\text{O}$ and the average vertical velocity (ω , hPa/s) at 4 pressure levels between 300 hPa and 600 hPa over a grid box of $75^\circ\text{E}\text{--}77.5^\circ\text{E}$, $7.5^\circ\text{N}\text{--}12.5^\circ\text{N}$ (Supplementary Fig. 1b), a linear correlation coefficient of 0.47 ($P < 0.001$) is observed up to the time of monsoon withdrawal. Recent studies point out the equal contributions of both convective and stratiform clouds in the Maximum

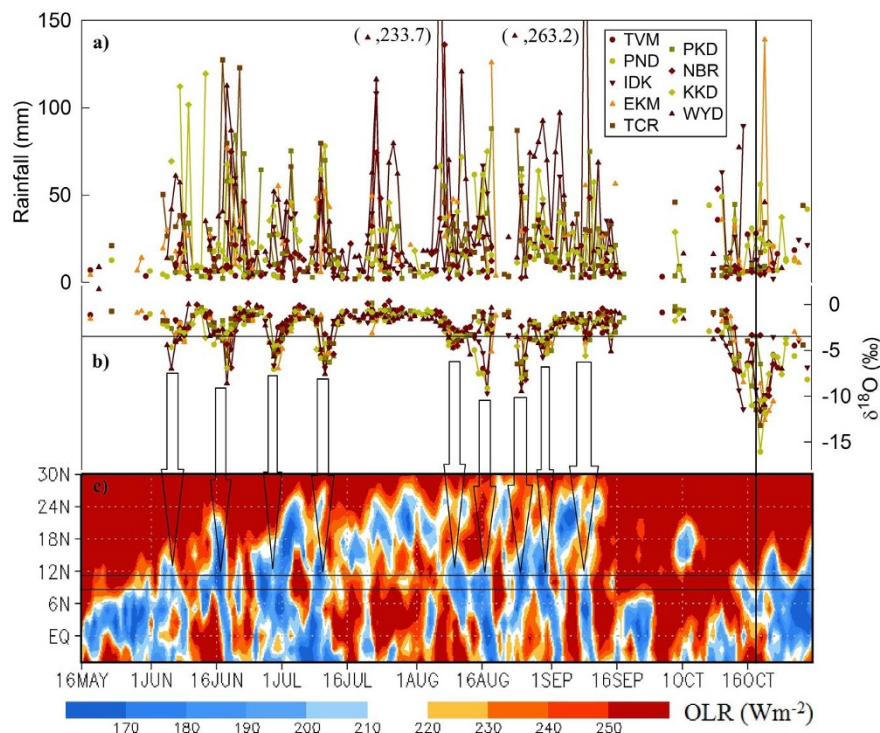


Figure 2 | Time series of the amount & $\delta^{18}\text{O}$ of rain and convective activity. (a) Time series of measured amount of daily rain (mm), (b) rain $\delta^{18}\text{O}$ (‰) relative to V-SMOW (scale on the right), and (c) Hovmöller diagram of average NOAA interpolated OLR over 65°E – 77.5°E . Rain events with $\delta^{18}\text{O}$ below -3.4‰ (amount weighted mean of all $\delta^{18}\text{O}$ values shown as solid line) corresponding to low values of OLR are shown by vertical arrows. Solid parallel lines in (c) depict the latitude range of the sampling stations. The vertical line indicates date of monsoon withdrawal. For station abbreviations see caption to Fig. 1. Plots produced by licensed Sigma plot and GrADS.

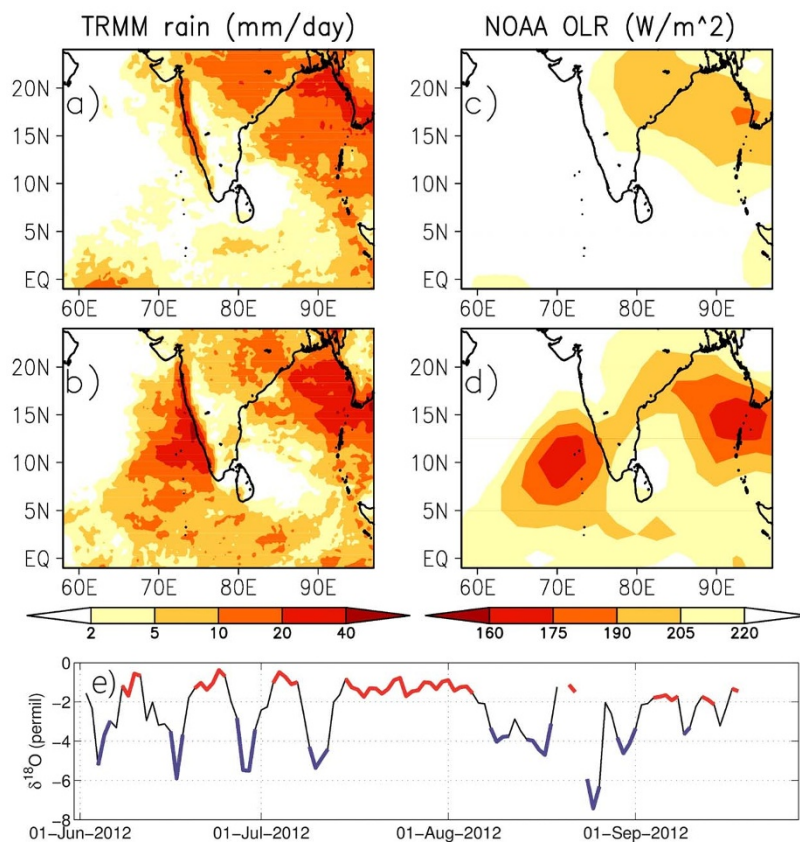


Figure 3 | Co-occurrence of large scale convection and isotopically depleted rain. Composite of rainfall (TRMM 3B42) and OLR (NOAA) pattern during high ^{18}O depletion (b,d) and low ^{18}O depletion (a,c) rain events. (e) Shows the days chosen to plot the composite of high ^{18}O depletion (blue) and low ^{18}O depletion (red) rain events. Maps plotted using GrADS.

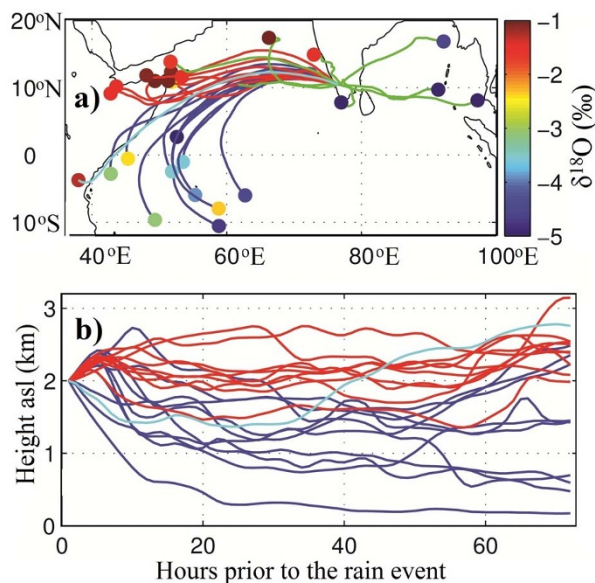


Figure 4 | Back trajectory analyses. (a) Three-days back trajectory to the mean location of sampling stations ($\sim 10.50^{\circ}\text{N}$, 76.50°E), derived from HYSPLIT model, for low ^{18}O depletion events (red lines), high ^{18}O depletion events (blue lines) and rain events during October (green lines), the month of monsoon withdrawal. Cyan line shows the back trajectory ending on 25th July, when low ^{18}O depletion events of heavy rainfall occurred in the absence of organised convection. The filled circles indicate the position of the air mass 72 hours prior to rain, and their colours indicate the $\delta^{18}\text{O}$ of rain at the final station (plotted at the initial point to avoid clustering at the end point); refer to colour code on the right. (b) Change in the height of the air mass en-route during high ^{18}O depletion (blue) and low ^{18}O depletion events (red), and on during 25th July (cyan) to the mean cloud base altitude at the sampling station (2 km). Maps plotted using licensed MATLAB.

Cloud Zone (MCZ) in determining the rainfall²⁰. Large spatial extent of stratiform cloud leads⁸ to mesoscale subsidence of depleted background vapour into the sub-cloud layer. ^{18}O depletion of stratiform clouds by this mixing of environmental air could also be an additional reason for the observed variability of rain $\delta^{18}\text{O}$. The ^{18}O depleted remnant vapour after the condensation also reaches the sub-cloud layer along with the mesoscale subsidence. During the convective updraft, this vapour is also taken up into the cloud^{8,9} from the sub-cloud layer and thus the rain becomes more depleted in ^{18}O . Hence, for large scale convective events, along with the other factors, recycling of isotopically depleted vapour from stratiform clouds during the MCZ activity also leads to the rain ^{18}O depletion.

During ISM, equatorially asymmetric pressure pattern leads to cross equatorial flow, also known as the Low Level Jet Stream (LLJ), which connects the Mascarene High in the Southern Hemisphere and the Monsoon Trough and transports moisture from the southern Indian Ocean to south Asia²¹. Intra seasonal variability of LLJ is also seen associated with the active/break cycles of ISM as per the pressure fluctuation between the two hemispheres²¹. Back trajectory analysis (see methods) shows that during days of higher ^{18}O -depletion, air mass travels longer distances from maritime locations from the south of the equator (Fig. 4a). In contrast, during the 3 days prior to the low ^{18}O -depletion events, the air mass moves zonally from the western Arabian Sea, as well as the inland locations of northern Somalia. This underscores the importance of location of vapour source and the track the air mass has followed in determining the rain $\delta^{18}\text{O}$. The possible reason for the high ^{18}O depletion in rain could also be due to (i) the difference in ^{18}O content of the marine source (e.g., southern Indian Ocean) and (ii) the cloud process along the trajectory before reaching the site of observation.

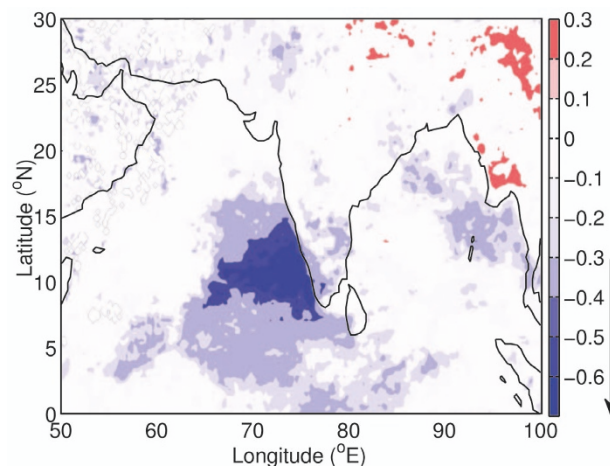


Figure 5 | Spatial correlation pattern of the daily average $\delta^{18}\text{O}$ of rain at all stations with the TRMM3B42 rainfall over the south Asian region at each $0.25^{\circ} \times 0.25^{\circ}$ grid for the period June to mid Oct. Values statistically significant at 0.001 level ($R > 0.30$) are indicated on the right with an arrow. Map plotted using licensed MATLAB.

An anomalous high rain event occurred during 18–28th July with low ^{18}O -depletion all over Kerala. The rain amount was quite high in many stations, particularly in the north. Organized convective activity was absent (included in the composite plots, Fig. 2c and Fig. 3a). Yet, the location of origin of the air mass (Fig. 4a) does not show significant difference (taking into account the associated model uncertainty) from those during high ^{18}O -depletion rain events. Air mass back trajectory of 25th July shows a descending motion up to 1.5 km (above m.s.l) till the previous 30 hours and subsequently an ascending motion (Fig. 4b). Therefore the dominant vapour source is likely confined to the atmosphere over the Arabian Sea (with little contribution from south of the equator), though the parcel had an apparent cross equatorial flow. Thus, along with the absence of large scale clouds during this event, this could also be a reason for the observed anomaly.

The daily amount-weighted all-station average $\delta^{18}\text{O}$ of rain and grid-wise ($0.25^{\circ} \times 0.25^{\circ}$) daily TRMM-derived rainfall shows a statistically significant ($R > 0.30$; $P > 0.001$) negative correlation over the south eastern Arabian Sea, including the Kerala coast (Fig. 5). The spatial correlation pattern is similar to the OLR and TRMM rainfall pattern during the high ^{18}O depletion events (Fig. 3b & 3d). This reinforces our conclusion that this negative relationship is not due to ‘amount effect’ (which is local) but rather due to large scale convection and the cloud spread.

After a dry period from mid September to 8th October, rain got established again. This was the period of monsoon withdrawal and the change in wind direction now brought moisture from Bay of Bengal (BoB). The rain $\delta^{18}\text{O}$ was much more depleted. The suggested^{6,12,22} reasons are: (i) the air mass travelled a longer distance from the BoB, effectively depleting the rain ^{18}O over Kerala, due to rainfall extraction *en route* (the continental effect), (ii) Relatively lower $\delta^{18}\text{O}$ of surface BoB due to seasonal runoff from the Ganga-Brahmaputra river system.

To summarise, the presence of large scale cloud bands during ISM leads to a marked ^{18}O -depletion in the monsoon rain. This signature of convective activity is well captured in rain $\delta^{18}\text{O}$ rather than in the local rainfall amount. This is confirmed by an analysis of the spatial pattern of clouds using OLR and the TRMM derived rainfall. Intense cloud activity with large spatial extent is associated with a strong cross equatorial flow and high moist air convergence over Kerala during all the high ^{18}O -depletion rain events. Analyses of proxies of convection such as OLR, vertical wind velocity and the air mass



back trajectory show high moisture convergence and heavy convection in the southern Peninsular India which can effectively take the recycled high ^{18}O depletion moisture from the sub cloud layer. Thus paleomonsoon proxies such as teak tree cellulose from Kerala may be interpretable in terms of the degree of large scale convective activity during the summer monsoon rather than the amount of monsoon rainfall.

Methods

Sampling and isotopic analysis. The protocol proposed by International Atomic Energy Agency (IAEA) was used for sample collection (<http://www-naweb.iaea.org/napc/ih>). Using a funnel and a carbuoy, rainfall was collected everyday at 3.30 am (UT) and transferred to leak-proof plastic bottles. Isotopic analyses of the samples were done with a Thermo Finnigan Delta V plus continuous flow isotope ratio mass spectrometer. CO_2 equilibration method was adopted for the sample $\delta^{18}\text{O}$ analysis²³. All of the measurements were performed with 1σ external precision of $\pm 0.1\text{‰}$. The precision and accuracy of the measurements were monitored by using an internal laboratory water standard, NARM (a large batch of Narmada River water with a $\delta^{18}\text{O}$ of -4.7‰ relative to V-SMOW). We also participated in the Fourth IAEA inter-laboratory comparison for oxygen isotopic analysis of water²⁴, and values reported by us are in good agreement with the IAEA consensus values.

Monsoon performance in 2012. India Meteorological Department (IMD) defines the onset of ISM as the abrupt increase in the rainfall amount in the south-western coast of peninsular India with a threshold amount of rainfall (at least 2.5 mm each for two consecutive days) recorded in at least 9 out of 14 stations. A certain minimum value for OLR and the westerly wind strength in the domain has also been considered for the declaration of the onset (<http://www.imd.gov.in/section/nhac/dynamic/mok.pdf>, accessed on 02/05/2013). In 2012, though the monsoon rainfall had started in 2 stations by 30th May itself, rainfall did not establish well in all the stations until 5th June, declared as the date of onset. Similarly, although the withdrawal of the monsoon was declared on 18th October, 2012¹⁶, continuous rain was recorded even after 18th October.

Data sources. Daily rainfall data from TRMM 3B42 with a spatial resolution of $0.25^\circ \times 0.25^\circ$ is utilized for the identification of larger scale spatial pattern of rainfall during the monsoon season. NOAA interpolated Outgoing Longwave Radiation (OLR) data with a spatial resolution of 2.5° latitude \times 2.5° longitude and a temporal resolution of 24 hrs is used to identify the extent of clouds and their propagation²⁵ and the MERRA (Modern-Era Retrospective Analysis for Research and Applications) vertical velocity data between 600 to 300 mb levels are utilized for the analysis of convective activity²⁶. The HYSPLIT (Hybrid Single-Particle Lagrangian Integrated Trajectory)²⁷ model is used for air mass back trajectory analysis for the 72 hrs prior to the rain occurrence.

- Managave, S. R. & Ramesh, R. in *Handbook of Environmental Isotope Geochemistry* (ed Baskaran, M.) Ch. 38, 811–833 (Springer-Verlag, Berlin, 2011).
- Managave, S. R., Sheshshayee, M. S., Bhattacharya, A. & Ramesh, R. Intra-annual variations of teak cellulose $\delta^{18}\text{O}$ in Kerala, India: implications to the reconstruction of past summer and winter monsoon rains. *Clim. Dynam.* **37**, 555–567 (2010).
- Yadava, M. G. & Ramesh, R. Significant long term periodicities in the proxy record of the Indian monsoon rainfall. *New. Astron.* **12**, 544–555 (2007).
- Sinha, A. *et al.* A 900 year (600 to 1500 A.D.) Record of the Indian summer monsoon precipitation from the core monsoon zone of India. *Geophys. Res. Lett.* **34**, L16707 (2007).
- Dansgaard, W. Stable isotopes in precipitation. *Tellus* **16**, 436–468 (1964).
- Yurtsever, R. & Gat, J. R. in *Stable Isotope Hydrology: Deuterium and Oxygen 18 in the Water Cycle. Technical Report Series*, IAEA Vienna, **210**, 103–142 (1981).
- Yadava, M. G. & Ramesh, R. Monsoon reconstruction from radiocarbon dated tropical Indian speleothems. *Holocene* **15**, 48–59 (2005).
- Kurita, N. Water isotopic variability in response to mesoscale convective system. *J. Geophys. Res-Atmos* **118**, 10376–10390 (2013).
- Risi, C., Bony, S. & Vimeux, F. Influence of convective processes on the isotopic composition ($\delta^{18}\text{O}$ and δD) of precipitation and water vapor in the tropics: 2. Physical interpretation of the amount effect. *J. Geophys. Res-Atmos* **113**, 1–12 (2008).
- Warrier, C. U. *et al.* Isotopic characterization of dual monsoon precipitation – evidence from Kerala, India. *Curr. Sci.* **98**, 1487–1495 (2010).
- Yadava, M. G., Ramesh, R. & Pandarinath, K. A positive “amount effect” in the Sahayadri (Western Ghats) rainfall. *Curr. Sci* **93**, 560–564 (2007).

- Breitenbach, S. F. M. *et al.* Strong influence of water vapor source dynamics on stable isotopes in precipitation observed in Southern Meghalaya, NE India. *Earth. Planet. Sci. Lett.* **292**, 212–220 (2010).
- Sikka, D. R. & Gadgil, S. On the maximum cloud zone and the ITCZ over Indian longitudes during the southwest monsoon. *Mon. Weather Rev.* **108**, 1840–1853 (1980).
- Gadgil, S. The Indian Monsoon and its variability, *Annual Review of Earth. Planet. Sci. Lett.* **31**, 429–467 (2003).
- Joseph, P. V., Simon, A., Nair, V. G. & Thomas, A. Intra-Seasonal Oscillation (ISO) of south Kerala rainfall during the summer monsoons of 1901–1995. *J. Earth. Syst. Sci.* **113**, 139–150 (2004).
- Pai, D. S. & Bhan, S. Monsoon Report 2012. *Monsoon Monograph, India Meteorological Department* 1–193 (2012).
- Rajendran, K., Kitoh, A., Srinivasan, J., Mizuta, R. & Krishnan, R. Monsoon circulation interaction with Western Ghats orography under changing climate. *Theor. Appl. Climatol.* **110**, 555–571 (2012).
- Kurita, N. *et al.* Intraseasonal isotopic variation associated with the Madden-Julian Oscillation. *J. Geophys. Res-Atmos* **116**, 1–20 (2011).
- Midhun, M., Lekshmy, P. R. & Ramesh, R. Hydrogen and oxygen isotopic compositions of water vapor over the Bay of Bengal during monsoon. *Geophys. Res. Lett.* **40**, 6324–6328 (2013).
- Chattopadhyay, R., Goswami, B. N., Sahai, A. K. & Fraedrich, K. Role of stratiform rainfall in modifying the northward propagation of monsoon intraseasonal oscillation. *J. Geophys. Res* **114**, D19114 (2009).
- Wang, B. *The Asian Monsoon* (Springer 2006).
- Singh, A., Jani, A. R. & Ramesh, R. Spatiotemporal variations of the $\delta^{18}\text{O}$ –salinity relation in the northern Indian Ocean. *Deep Sea Res., Part I* **57**, 1422–1431 (2010).
- Epstein, S. & Mayeda, T. Variation in O^{18} content of waters from natural sources. *Geochim. Cosmochim. Acta* **4**, 213–224 (1953).
- Ahmad, M. *et al.* Final Report on Fourth interlaboratory comparison exercise for δ^{H} and $\delta^{18}\text{O}$ analysis of water samples. IAEA (WICO2011) (2012).
- Liebmann, B. & Smith, C. A. Description of a Complete (Interpolated) Outgoing Longwave Radiation Dataset. *B. Am. Meteorol. Soc.* **77**, 1275–1277 (1996).
- Rienecker, M. M. *et al.* MERRA-NASA’s Modern-Era Retrospective Analysis for Research and Application. *J. Climate (MERRA special collection)* **24**, 3624–3648 (2011).
- Draxler, R. R. & Rolph, G. D. HYSPLIT (Hybrid Single-Particle Lagrangian Integrated Trajectory) Model access via NOAA ARL READY Website (<http://ready.arl.noaa.gov/HYSPLIT.php>). NOAA Air Resources Laboratory, Silver Spring, MD (2014).

Acknowledgments

We thank PV Ravisankar, Lathika Sreenivas, Abraham Baby, Sugunan, Rekha Ajayaghosh, Sivadasan, Adarsh, Smruthy Sinjith, Asokan and PC Sreedharan for help in collecting the samples. The TRMM 3B42 data were obtained from the National Aeronautics and Space Administration Goddard Earth Sciences Data and Information Service Center. This project was funded by the ISRO-GBP, Government of India. We thank the referees for their critical comments.

Author contributions

R.R., P.R.L. and M.M. designed the study, P.R.L. and M.M. coordinated the sampling network, and R.R. and P.R.L. jointly wrote the manuscript. P.R.L. performed the bulk of isotopic measurements. M.M. and R.A.J. helped with measurements.

Additional information

Supplementary information accompanies this paper at <http://www.nature.com/scientificreports>

Competing financial interests: The authors declare no competing financial interests.

How to cite this article: Lekshmy, P.R., Midhun, M., Ramesh, R. & Jani, R.A. ^{18}O depletion in monsoon rain relates to large scale organized convection rather than the amount of rainfall. *Sci. Rep.* **4**, 5661; DOI:10.1038/srep05661 (2014).



This work is licensed under a Creative Commons Attribution-NonCommercial-NoDerivs 4.0 International License. The images or other third party material in this article are included in the article’s Creative Commons license, unless indicated otherwise in the credit line; if the material is not included under the Creative Commons license, users will need to obtain permission from the license holder in order to reproduce the material. To view a copy of this license, visit <http://creativecommons.org/licenses/by-nc-nd/4.0/>